

# Self-Assembled Monolayer Growth of Octadecylphosphonic Acid on Mica

John T. Woodward,<sup>†</sup> Abraham Ulman,<sup>‡</sup> and Daniel K. Schwartz<sup>\*,†</sup>

Department of Chemistry, Tulane University, New Orleans, Louisiana 70118,  
and Department of Chemistry, Polytechnic University, Brooklyn, New York 11201

Received November 27, 1995<sup>®</sup>

Self-assembled monolayers are formed by exposing freshly cleaved mica to a solution of octadecylphosphonic acid in tetrahydrofuran. Atomic force microscope images of samples immersed in solution for varying exposure times show that prior to forming a complete monolayer the molecules aggregate into dense islands ( $1.8 \pm 0.2$  nm high) on the surface. The islands have a compact, rounded morphology. The cosine of the contact angle between hexadecane and the partial monolayers has an approximately linear dependence on coverage. However, the cosine of the contact angle of water decreases linearly to about 50% coverage (the percolation threshold of the phosphonate islands) and then appears to saturate.

## Introduction

Tremendous progress toward the understanding of self-assembled monolayer (SAM) structure has been made over the last few years due to excellent work by several research groups. The majority of this work has focused on the alkanethiol/Au(111) SAM system<sup>1-15</sup> with a significant amount of work on alkyltrichlorosilane (or triethoxysilane) SAM's.<sup>16-19</sup>

X-ray and helium diffraction<sup>4,8,10,14</sup> combined with STM measurements<sup>1-3,7,9-11,15</sup> have discovered a wealth of structural phases on thiol/gold SAM's as a function of chain length and temperature and firmly placed SAM's in their rightful place as examples of molecular epitaxy. This particular system has limitations, however, with respect to its direct technological applicability as well as its suitability as a model system for scanning probe micros-

copy and kinetic studies. The chemical process of attachment between the thiol and gold is extremely specific and not well understood. At present, in fact, there is a controversy as to whether the attached species is a thiol, a thiolate, or even a disulfide. In addition, there is the matter of the omnipresent "pits"<sup>2,7,12,15</sup> found on the surface after thiol deposition, implying, again, that the reaction is not well understood. Also, the difficulties involved in preparing and imaging the substrates and films in the thiol/gold system make a systematic study of the growth kinetics and morphology prohibitively time-consuming. As a result, direct kinetic studies of the monolayer structure during growth have not been performed. We feel that there is a need for studies of a system in which (1) the attachment chemistry is fairly general and the attachment group can be systematically varied, (2) substrates are macroscopically large and flat, easily prepared, and imaged in ambient conditions, and (3) growth kinetics and morphology can be easily studied using *ex situ* and *in situ* techniques.

In previous work, we examined SAM formation of octadecyltrichlorosilane (OTS) on mica with the AFM.<sup>17</sup> We prepared a series of incomplete monolayers, immersing substrates for varying periods of time, removing them and rinsing, and then imaging the film under ambient conditions. The monolayer appeared to grow by the formation of self-similar (fractal) islands with a height consistent with a fully-extended OTS molecule (2.5 nm). Coverage kinetics and changing island morphology with immersion time indicated two regimes: an initial fast growth period (with morphology consistent with diffusion-limited aggregation) followed by a crossover to an adsorption-limited regime as the domains filled in. The final film retained faint "scars" reminiscent of the growth domains. This established the direct relation between growth mechanism and final film structure. The particular mechanism observed, however, was directly linked to the ability of the OTS molecules to polymerize. A more disturbing lingering question about the work was the actual relevance of the films removed from solution to the monolayer before removal. Are the partial films actually representative of the growth of the monolayer in solution, or does the process of removing the partial film from solution cause significant changes in the structure? Since there have been no further direct kinetic studies of SAM growth, these and other important questions remain unanswered.

We propose, in this manuscript, a model system for such kinetic studies. We were motivated by earlier work using

\* To whom correspondence should be addressed. FAX: 504-865-5596. Phone: 504-865-5573. E-mail: dks@mailhost.tcs.tulane.edu.

<sup>†</sup> Tulane University.

<sup>‡</sup> Polytechnic University.

<sup>®</sup> Abstract published in *Advance ACS Abstracts*, June 15, 1996.

(1) Widrig, C. A.; Alves, C. A.; Porter, M. D. *J. Am. Chem. Soc.* **1991**, *113*, 2805.

(2) Alves, C. A.; Smith, E. L.; Porter, M. D. *J. Am. Chem. Soc.* **1992**, *114*, 1222.

(3) Kim, Y.-T.; Bard, A. J. *Langmuir* **1992**, *8*, 1096.

(4) Camillone, N., III; Chidsey, C. E. D.; Eisenberger, P.; Fenter, P.; et al. *J. Chem. Phys.* **1993**, *99*, 744.

(5) Chailapakul, O.; Sun, L.; Xu, C.; Crooks, R. M. *J. Am. Chem. Soc.* **1993**, *115*, 12459.

(6) Dubois, L. H.; Zegarski, B. R.; Nuzzo, R. G. *J. Chem. Phys.* **1993**, *98*, 678.

(7) Edinger, K.; Golzhauser, A.; Demota, K.; Woll, C.; et al. *Langmuir* **1993**, *9*, 4.

(8) Fenter, P.; Eisenberger, P.; Liang, K. S. *Phys. Rev. Lett.* **1993**, *70*, 2447-2450.

(9) Pan, J.; Tao, N.; Lindsay, S. M. *Langmuir* **1993**, *9*, 1556.

(10) Camillone, N.; Eisenberger, P.; Leung, T. Y. B.; Schwartz, P.; et al. *J. Chem. Phys.* **1994**, *101*, 11031-11036.

(11) Poirier, G. E.; Tarlov, M. J.; Rushmeier, H. E. *Langmuir* **1994**, *10*, 3383-3386.

(12) Schönenberger, C.; Sondag-Huethorst, J. A. M.; Jorritsma, J.; Fokkink, L. G. J. *Langmuir* **1994**, *10*, 611.

(13) Stranick, S. J.; Parikh, A. N.; Tao, Y.-T.; Allara, D. L.; et al. *J. Phys. Chem.* **1994**, *98*, 7636.

(14) Li, J.; Liang, K. S.; Camillone, N.; Leung, T. Y. B.; et al. *J. Chem. Phys.* **1995**, *102*, 5012.

(15) Poirier, G. E.; Tarlov, M. J. *J. Phys. Chem.* **1995**, *99*, 10966-10970.

(16) Brzoska, J. B.; Shahidzadeh, N.; Rondelez, F. *Nature* **1992**, *360*, 719.

(17) Schwartz, D. K.; Steinberg, S.; Israelachvili, J.; Zasadzinski, J. A. N. *Phys. Rev. Lett.* **1992**, *69*, 3354-3357.

(18) Parikh, A. N.; Allara, D. L.; Azouz, I. B.; Rondelez, F. *J. Phys. Chem.* **1994**, *98*, 7577-7590.

(19) Xiao, X.-D.; Liu, G.-Y.; Charych, D. H.; Salmeron, M. *Langmuir* **1995**, *11*, 1600-1604.

octadecylphosphate<sup>20</sup> to try octadecylphosphonic acid (OPA) as a molecule for self-assembly on mica. Mica substrates are inexpensive and easily prepared, and the atomically flat, single-crystal surface is ideal for scanning force microscopy studies. The attachment chemistry is not extremely specific, and synthesis of functionalized molecules is straightforward.

### Experimental Section

Octadecylphosphonic acid ( $\text{CH}_3(\text{CH}_2)_{17}\text{PO}_3\text{H}_2$ ) was prepared by the Michaelis–Arbuzov reaction of 1-bromooctadecane ( $\text{CH}_3(\text{CH}_2)_{17}\text{Br}$ ) with triethyl phosphite ( $(\text{C}_2\text{H}_5\text{O})_3\text{P}$ ) both obtained from Kodak.  $\text{CH}_3(\text{CH}_2)_{17}\text{Br}$  (10 mmol) and  $(\text{C}_2\text{H}_5\text{O})_3\text{P}$  (30 mmol) were refluxed at 150 °C for 6 h, the solution was cooled to room temperature, and about 40 mL of concentrated (36.5–38%) aqueous HCl solution was added. Heating was resumed at 100 °C overnight (16 h). The solution was cooled to room temperature, 10 mL of water was added, and the solid was filtered. Crystallization from heptane–isopropanol gave white crystals.

Tetrahydrofuran (99.9%, Fisher Scientific, Pittsburg, PA) was used as a solvent. The water used as the subphase for the Langmuir isotherms and for contact angle measurements was from a Millipore Milli-Q UV+ (Bedford, MA). Hexadecane (99%, Aldrich) was also used for contact angle measurements. Isotherms of Langmuir monolayers of OPA were measured on a NIMA (Coventry, England) model 611 Langmuir trough. The film was deposited onto the water surface (held at  $22.0 \pm 0.2$  °C) from a 0.1 mM solution of OPA in THF and allowed to relax for 5 min before being compressed at 50  $\text{cm}^2/\text{min}$ .

To enable us to make several SAM samples simultaneously, a substrate holder was fashioned by making six razor cuts, separated by 6 mm, in a 4 mm o.d. Teflon tube. A section of glass tubing with two notches supported the substrate holder above a stirring bar in the solution. A 12.5 mm diameter disk of freshly-cleaved mica was placed in each of the razor cuts. The substrates were submerged in a 0.2 mM solution of OPA in THF and removed at intervals of 1, 2, 5, 10, 30, and 120 min. Upon removal the samples were rinsed in pure THF for 30 s and blown dry with a dry nitrogen stream. Two sets of samples were made using the same solution.

The samples were imaged with a Nanoscope III atomic force microscope (Digital Instruments, Santa Barbara, CA). All images were taken in contact mode using silicon nitride tips. Surface coverage was calculated using the height histogram of a given image. Since the peak in the histogram corresponding to pixels that are part of islands was often asymmetric because of tip convolution effects at island edges (in particular, this peak has a prominent shoulder), we computed the surface coverage by doubling the integrated intensity of the “high” half of this peak. The average of and uncertainty in island height were also calculated using these histograms. Contact angle measurements were made using a custom-built contact angle goniometer. For measurements of the so-called “static” contact angle, we followed a procedure described by Bain et al.<sup>21</sup> in which a 1  $\mu\text{L}$  drop was formed at the end of a needle and brought into contact with the surface. The needle was removed and the contact angle measured. Results were reproducible to within  $\pm 2^\circ$ . To measure advancing or receding contact angles, the angle was measured as a microliter syringe was used to add liquid to or remove liquid from the drop.

### Results and Discussion

An isotherm of a Langmuir monolayer of OPA on the water surface is shown in Figure 1. The isotherm indicates a liquid phase beginning at 22.0  $\text{\AA}^2/\text{molecule}$  and a transition to a less compressible phase at 18.8  $\text{\AA}^2/\text{molecule}$  and 15.0 mN/m. The compressibility of the high-pressure phase is 0.0034 mN/m. The solid phase collapses at a pressure of 37–40 mN/m. A previously published isotherm<sup>22</sup> achieved a collapse pressure of 53 mN/m; however,

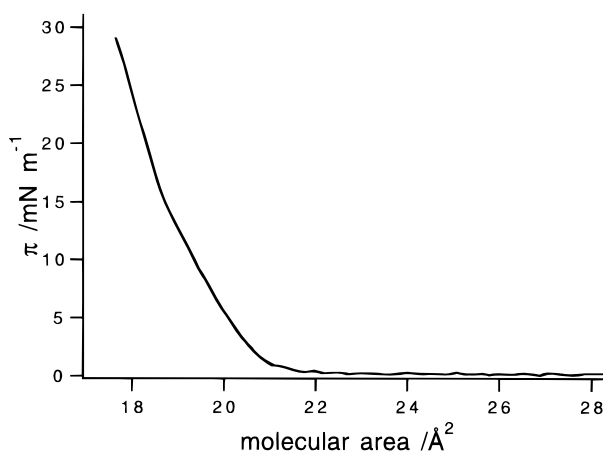


**Figure 1.** Isotherm of octadecylphosphonic acid on a water subphase at 22 °C. Note two kinks (i.e. changes in slope) in the isotherm at 21  $\text{\AA}^2/\text{mol}$  and 18.8  $\text{\AA}^2/\text{mol}$ .

collapse pressures are notoriously dependent on the details of experimental procedure such as compression speed. The authors make no mention of a clearly-defined liquid–solid transition, and data in the region are obscured by another isotherm in the published manuscript. Their value for the compressibility of 0.0035 mN/m is in good agreement with our own in the solid phase.

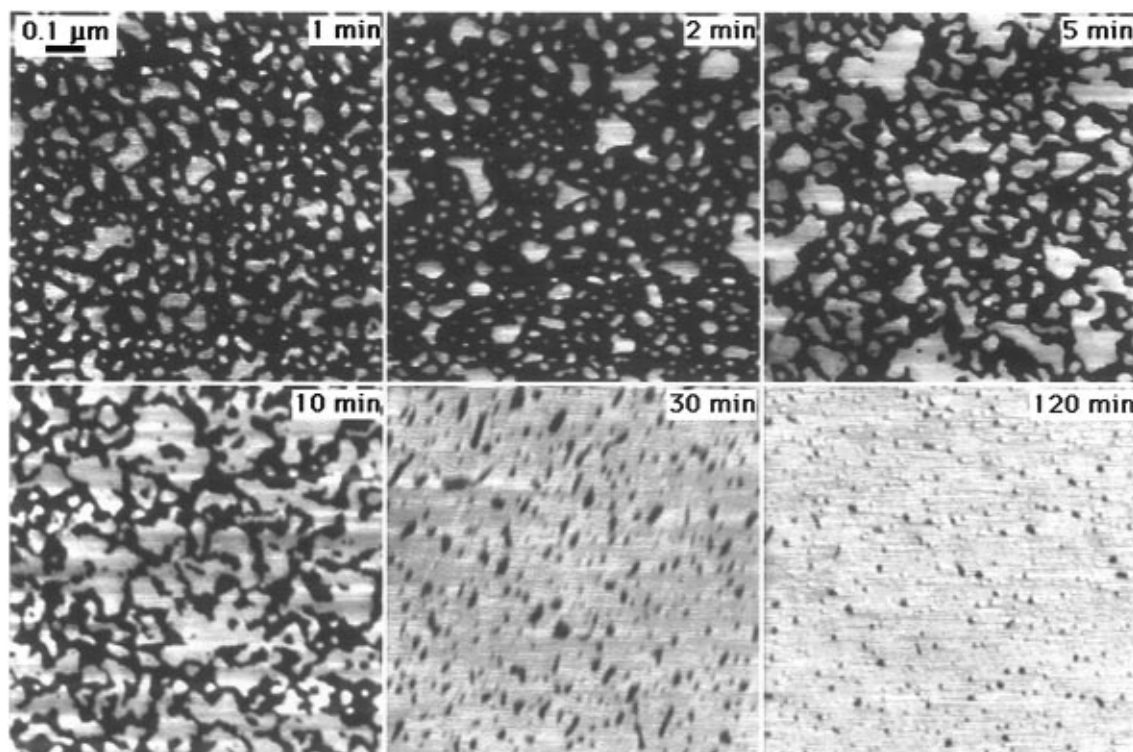
The atomic force microscope images clearly show that the OPA molecules aggregate to form islands on the mica surface during the early stages of monolayer formation. Figure 2 shows images of samples that were in solution for 1, 2, 5, 10, 30, and 120 min. These images are typical of images obtained from at least two macroscopically-separated regions on each sample and show the typical behavior of coverage versus time we have observed on 11 sets of samples. The control experiment of immersing the mica in solvent alone yielded flat featureless mica surfaces. We can observe the typical atomic-resolution crystal structure of mica in the low areas between the islands. In addition, when we scratch away an island by increasing the force exerted by the tip, the area exposed by the scratching is at the same level as the low areas surrounding the islands. We conclude that the low areas correspond either to bare mica or to an extremely thin and delicate layer of adsorbate molecules. Initially, small islands ( $\leq 10$  nm) form, as seen in the 1 and 2 min films. The small islands are generally round, in contrast to the aggregates observed in OTS growth, which are fractal. We believe this is a consequence of the qualitative difference in the attachment chemistry of the two systems. Since OTS cross-links covalently with other molecules, a molecule essentially “sticks” to whatever part of an island with which it first comes in contact, thus the similarity to diffusion-limited aggregation and the fractal morphology. The round islands observed in the partial OPA monolayers imply that the attachment to the islands is not irreversible and that rearrangement and/or annealing can take place. The fact that the preferred shape for the small domains is round implies that there is a significant effective line tension between the islands and the “bare” areas. These islands increase in size and grow together, as seen in the 5 and 10 min films. Eventually, only small holes in the film remain and gradually fill in, as seen in the 30 and 120 min films.

Table 1 shows the percentage of the surface covered by the monolayer islands from the sample set shown in Figure 2 and the other set made with the same batch of solution. The level of reproducibility between the two data sets is typical of samples made from the same solution. However, the details of the kinetics were not as reproducible between

(20) Maoz, R.; Sagiv, J. *J. Colloid Interface Sci.* **1984**, *100*, 465.

(21) Bain, C. D.; Troughton, E. B.; Tao, Y.-T.; Evall, J.; et al. *J. Am. Chem. Soc.* **1989**, *111*, 321–335.

(22) Ries, H. E.; Cook, H. D. *J. Colloid. Sci.* **1954**, *9*, 535.



**Figure 2.** AFM images of a mica surface exposed to a 0.2 mM solution of octadecylphosphonic acid in tetrahydrofuran. The exposure times are noted on the images. All images are  $1 \mu\text{m} \times 1 \mu\text{m}$ , and the gray scale is 5.0 nm black to white with lighter areas higher than dark ones.

**Table 1**

time, min	run 1 coverage, %	run 2 coverage, %
1	$26 \pm 2$	$23 \pm 2$
2		$23 \pm 2$
5	$30 \pm 3$	$39 \pm 3$
10	$48 \pm 2$	$46 \pm 2$
30	$86 \pm 2$	$62 \pm 2$
120	$93 \pm 3$	$87 \pm 4$

samples made from separate batches of solution that were nominally the same concentration. We believe that the kinetics are quite sensitive to small variations in the concentration. In fact, a simple calculation predicts that the prefactor in the adsorption kinetics goes like the square of the concentration.<sup>23,24</sup> The coverage data actually represent a lower limit to the number of molecules adsorbed on the surface, since molecules that may be loosely attached between islands would not be counted by our image analysis procedure.

The height of the islands is  $1.8 \pm 0.2$  nm. As the length of a fully extend OPA molecule is 2.5 nm, this implies either that the hydrocarbon chain has a  $40^\circ$  tilt angle with respect to the surface or that the chain is significantly disordered. Assuming conservation of volume and a close-packed area/molecule of about  $18 \text{ \AA}^2$ , the film thickness implies an area/molecule of about  $25 \text{ \AA}^2$ . This area is somewhat larger than we would expect from comparison with the Langmuir monolayer isotherm which showed the onset of a condensed phase at  $22 \text{ \AA}^2/\text{molecule}$ .

As shown in Table 1, the smallest coverage we observe is approximately 25%. In fact, this is typical of all the monolayers made with the 0.2 mM solution, even for shorter immersion times than 1 min. Also, note that the coverage after 2 min is identical to that after 1 min. Since it is difficult to reconcile these kinetics with any theoretical

model of adsorption and/or growth kinetics,<sup>23–27</sup> we speculate that the observed coverage kinetics are not a simple consequence of adsorption from solution but also contain a component due to insertion and/or removal from the solution. For example, a dilute adsorbed monolayer at the solution/air interface could be transferred to the substrate during insertion or removal in analogy with Langmuir–Blodgett transfer. It is also possible that the removal from solution and rinsing could have affected the island morphology as well. Only *in situ* studies of monolayer growth will conclusively resolve this issue.

There is a systematic correlation between static contact angles of water and hexadecane and surface coverage as measured by AFM (see Figure 3). The contact angle of hexadecane increased gradually from about  $20^\circ$  on bare mica to about  $45^\circ$  on a fully-formed film while the contact angle of water increased from  $<3^\circ$  on mica to about  $90^\circ$ . The maximum contact angle of hexadecane ( $45^\circ$ ) compares favorably with those on well-formed thiolate monolayers.<sup>28</sup> However, the maximum static contact angle of water ( $89^\circ$ ) is  $20^\circ$  less than would be expected for water on a well-ordered methyl-terminated surface.<sup>29</sup> This is consistent with substantial chain disorder.<sup>29</sup>

The contact angles of hexadecane were stable for more than 5 min; however, those of water typically decreased by  $15^\circ$ – $20^\circ$  after the water drop remained on the surface for 5 min. This suggests that the monolayer is not extremely robust. In addition, a 5 min sonication in water reduced the contact angle of a fully formed film to  $55^\circ$ . The static contact angles of water were about  $5^\circ$  lower than the measured advancing contact angle. The receding contact angles of water, on the other hand, are extremely small, less than  $10^\circ$ , for both a 50% and a 90% covered

(25) Bartlett, M. C.; Evans, J. W. *Phys. Rev. B* **1992**, *46*, 12675.

(26) Bales, G. S.; Chozan, D. C. *Phys. Rev. B* **1994**, *50*, 6057.

(27) Ratsch, C.; Zangwill, A.; Smilauer, P.; Vvedensky, D. D. *Phys. Rev. Lett.* **1994**, *72*, 3194.

(28) Whitesides, G. M.; Laibinis, P. E. *Langmuir* **1990**, *6*, 87.

(29) Bain, C. D.; Whitesides, G. M. *Angew. Chem.* **1989**, *101*, 522.

(23) Frisch, H. L.; Mysels, K. J. *J. Phys. Chem.* **1983**, *87*, 3988–3990.  
(24) Mysels, K. J.; Frisch, H. L. *J. Colloid Interface Sci.* **1984**, *99*, 136–140.

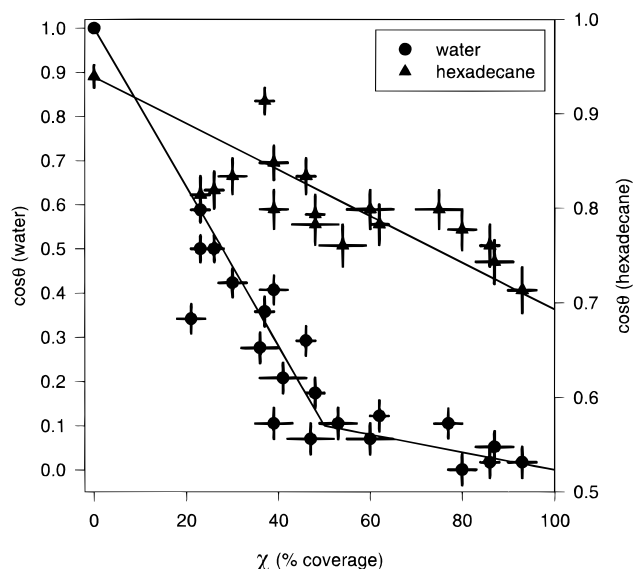


**Figure 3.** Cosine of the static contact angle of water and hexadecane versus the surface coverage measured using AFM. The left-hand vertical axis refers to water, and the right-hand axis refers to hexadecane. The solid line drawn through the hexadecane data is a best fit to a straight line assuming a linear dependence of surface free energy on coverage. The water data are not well described by a single straight line and seem to approximately saturate at about 50% coverage.

surface. Since we suspected that this was indicative of surface damage due to exposure to the water, we added water back to the drop after measuring the receding angle; the new advancing angle was only 10–20° less than the original advancing angle. This 10–20° difference is ascribed to possible surface damage; however, the remaining hysteresis is still very large.

The standard first approximation for the contact angle of a liquid in contact with a chemically heterogeneous surface composed of a fraction  $f_1$  of chemical groups of type 1 and a fraction  $f_2$  of groups of type 2 is the Cassie equation<sup>30–32</sup> (essentially a mean-field approximation)

$$\cos \theta = f_1 \cos \theta_1 + f_2 \cos \theta_2$$

where  $\theta_1$  and  $\theta_2$  are the contact angle of the pure, homogeneous type 1 and type 2 surfaces, respectively. In our case, this can be written

$$\cos \theta = \cos \theta_{\text{mica}} + \chi(\cos \theta_{\text{monolayer}} - \cos \theta_{\text{mica}})$$

where  $\chi$  is the fractional monolayer coverage. This implies a linear relationship between  $\cos \theta$  and  $\chi$ . It is interesting to compare our data to this phenomenological equation. Figure 3 shows a plot of  $\cos \theta$  versus  $\chi$  for hexadecane and water. Note that the vertical axis on the right corresponds to the hexadecane data. The hexadecane data are in reasonable agreement with the fit to a straight line. Since the water contact angles are not perfectly stable with time,

we must be careful about applying theories based on equilibrium thermodynamics. Nevertheless, it is interesting to note that they are not well described by a single line. They appear to decrease linearly to about 50% coverage where they essentially saturate. We have, therefore, drawn the best fit lines to the low- and high-coverage regions separately. We note that the coverage of 50% is the point where the islands of OPA percolate across the sample. It is possible that the advancing three-phase line of water could become pinned on these continuous islands. We cannot simply ascribe the contact angle behavior to film damage at the three-phase line, since the contact angle actually increases *more* quickly with coverage than predicted by the simple approximation given above. We would argue that hexadecane behaves differently, since the contact angles on covered and bare regions respectively are much closer to each other in value than for water. In any case, it is clear that the wetting of hexadecane is significantly more sensitive to inhomogeneity at these mesoscopic length scales than that of water. The only other theoretical form we have discovered for heterogeneous surfaces<sup>32</sup> is appropriate only for molecular-scale heterogeneity and, in fact, predicts values of  $\cos \theta$  slightly larger than those of the Cassie equation. Finally, we note that a more sophisticated analysis of contact angles on incomplete monolayers should consider additional factors such as the specific shape of the molecules in the wetting liquid and the morphology of defects present in the monolayer.

It is difficult to account for the possible effects of a low density of molecules that might be adsorbed between islands. So long as the density of such molecules remains constant with island coverage, the Cassie equation still predicts a linear relationship between  $\cos \theta$  and  $\chi$  with the data extrapolating to a value less than unity at zero coverage. This still does not describe the water data very well. However, we cannot rule out the possibility that the density or structure of molecules adsorbed between islands might change significantly with coverage.

### Conclusions

We have demonstrated that monolayers of OPA are adsorbed on mica from THF solution. AFM images of partially formed monolayers created at different exposure times show that the molecules on the surface aggregate into rounded islands, implying that rearrangement can take place and that the islands have a line tension. The height of the islands is 1.8 nm, implying that the alkyl chains are tilted or disordered and that the average area/molecule is approximately 25 Å<sup>2</sup>. The contact angle of hexadecane and water on the samples increases monotonically with increased surface coverage. The degradation of the water contact angle shows that the films are not robust. They are, however, useful as model systems for studying the structure and kinetics of the formation of self-assembled monolayers.

**Acknowledgment.** J.T.W. and D.K.S. acknowledge support from the Camille and Henry Dreyfus New Faculty Award Program and the Exxon Education Foundation and thank H. D. Sikes for the Langmuir monolayer isotherm measurements.

LA9510689

(30) Cassie, A. B. D. *Discuss. Faraday Soc.* **1952**, 75, 5041.

(31) Lamb, R. N.; Furlong, D. N. *J. Chem. Soc., Faraday Trans. 1* **1982**, 78, 61.

(32) Israelachvili, J. N.; Gee, M. L. *Langmuir* **1989**, 5, 288.